The Journal of Chemical Physics ARTICLE pubs.aip.org/aip/jcp

Low-temperature trapping of N_2 reduction reaction intermediates in nitrogenase MoFe protein–CdS quantum dot complexes

Cite as: J. Chem. Phys. 159, 235102 (2023); doi: 10.1063/5.0170405
Submitted: 2 August 2023 • Accepted: 24 November 2023 •
Published Online: 20 December 2023

Lauren M. Pellows,[1] Gregory E. Vansuch,[2] Bryant Chica,[2] Zhi-Yong Yang,[3] Jesse L. Ruzicka,[1] Mark A. Willis,[4] Andrew Clinger,[3] Katherine A. Brown,[2] Lance C. Seefeldt,[3] John W. Peters,[4,5] Gordana Dukovic,[1,6,7] David W. Mulder,[2,a)] and Paul W. King[2,7,a)]

AFFILIATIONS

[1] Department of Chemistry, University of Colorado Boulder, Boulder, Colorado 80309, USA
[2] Biosciences Center, National Renewable Energy Laboratory, Golden, Colorado 80401, USA
[3] Department of Chemistry and Biochemistry, Utah State University, Logan, Utah 84322, USA
[4] Institute of Biological Chemistry, Washington State University, Pullman, Washington 99163, USA
[5] Department of Chemistry and Biochemistry, University of Oklahoma, Norman, Oklahoma 73019, USA
[6] Materials Science and Engineering, University of Colorado Boulder, Boulder, Colorado 80303, USA
[7] Renewable and Sustainable Energy Institute (RASEI), University of Colorado Boulder, Boulder, Colorado 80303, USA

Note: This paper is part of the JCP Special Topic on The Physical Chemistry of Solar Fuels Catalysis.
[a)]**Authors to whom correspondence should be addressed:** david.mulder@nrel.gov and paul.king@nrel.gov

ABSTRACT

The biological reduction of N_2 to ammonia requires the ATP-dependent, sequential delivery of electrons from the Fe protein to the MoFe protein of nitrogenase. It has been demonstrated that CdS nanocrystals can replace the Fe protein to deliver photoexcited electrons to the MoFe protein. Herein, light-activated electron delivery within the CdS:MoFe protein complex was achieved in the frozen state, revealing that all the electron paramagnetic resonance (EPR) active E-state intermediates in the catalytic cycle can be trapped and characterized by EPR spectroscopy. Prior to illumination, the CdS:MoFe protein complex EPR spectrum was composed of a $S = 3/2$ rhombic signal ($g = 4.33$, 3.63, and 2.01) consistent with the FeMo-cofactor in the resting state, E_0. Illumination for sequential 1-h periods at 233 K under 1 atm of N_2 led to a cumulative attenuation of E_0 by 75%. This coincided with the appearance of $S = 3/2$ and $S = 1/2$ signals assigned to two-electron (E_2) and four-electron (E_4) reduced states of the FeMo-cofactor, together with additional $S = 1/2$ signals consistent with the formation of E_6 and E_8 states. Simulations of EPR spectra allowed quantification of the different E-state populations, along with mapping of these populations onto the Lowe–Thorneley kinetic scheme. The outcome of this work demonstrates that the photochemical delivery of electrons to the MoFe protein can be used to populate all of the EPR active E-state intermediates of the nitrogenase MoFe protein cycle.

INTRODUCTION

The biological reduction of dinitrogen (N_2) to ammonia (NH_3) and protons to dihydrogen (H_2) requires the ATP-dependent, sequential delivery of electrons from the Fe protein to the MoFe protein of nitrogenase.[1–3] Electron accumulation on the MoFe protein active site FeMo-cofactor leads to the formation of discrete E_n (n = 0, 1, 2, etc., electrons) states (Fig. 1), which are the intermediates of the N_2 reduction mechanism.[4,5] Important insights about the properties of E-states and the mechanism of nitrogenase N_2 reduction have come from interrogating Fe protein–MoFe protein complexes (both wild-type and variant proteins with amino acid substitutions) trapped during steady-state turnover.[5–14] The resulting compositions of paramagnetic, even numbered E-states

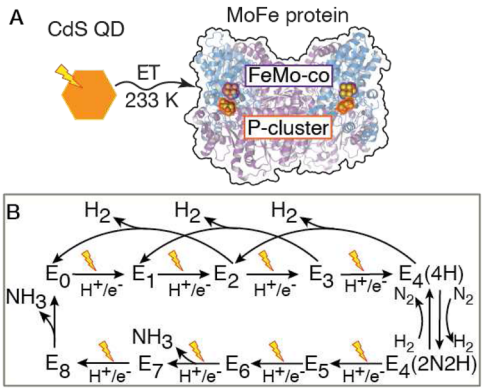

FIG. 1. Top: scheme of the light-driven process of electron delivery in CdS:MoFe protein complexes. Bottom: simplified Lowe–Thorneley kinetic scheme of N_2 reduction by nitrogenase.[16] Sequential delivery of electrons to the MoFe protein results in the reduction of the catalytic site FeMo-cofactor and the formation of intermediate E_n-states in the catalytic reduction of N_2 to NH_3 and H_2.

have been analyzed by electron paramagnetic resonance (EPR) spectroscopy, leading to a mechanistic model of the N_2 reduction reaction (Fig. 1).[5,15]

Electron delivery to the MoFe protein and catalysis of the N_2 reduction reaction can also be achieved with CdS nanorods and quantum dots (referred to as CdS QD, Fig. 1) replacing the Fe protein.[17,18] In this system, photoexcitation rates of QDs can be used to control electron flux into the MoFe protein. Herein, controlled illumination of QD:MoFe protein complexes in the frozen state was used to populate E-states in the pre-steady state. Illumination-dependent reduction of the MoFe protein was tracked by monitoring the reduction of the resting state, E_0, to EPR active, even numbered E-states, which were quantified and mapped onto the Lowe–Thorneley kinetic scheme.

RESULTS AND DISCUSSION

Photochemical reduction of the MoFe protein was tested with two QD preparations that differed in diameter. The ability of QDs to photochemically activate the MoFe protein was tested in reactions prepared under 1 atm of N_2 and illuminated at T = 298 K to measure NH_3 production (see Figs. S1 and S2 and Table S1 of the supplementary material).[19] Under these conditions, the complexes catalyzed NH_3 production with a turnover frequency (TOF) of 2.3–3.7 ± 1.0 mol NH_3 (mol MoFe protein)$^{-1}$ min^{-1}, within the range previously measured for other CdS:MoFe protein complexes.[17,18] The variation in TOF exemplifies the sensitivity to properties of CdS nanocrystals, the illumination intensity of the reactions, and the quantum efficiency of electron transfer (QEET).[17,18,20–22]

We have demonstrated that MoFe protein reaction intermediates can be trapped by illuminating CdS:MoFe protein complexes in the frozen state, T ~ 230–260 K, which allows electron delivery from CdS to the MoFe protein while minimizing turnover and formation of reaction products (i.e., NH_3 and H_2).[19,23,24] Here, CdS:MoFe protein complexes were tested under a series of reaction conditions

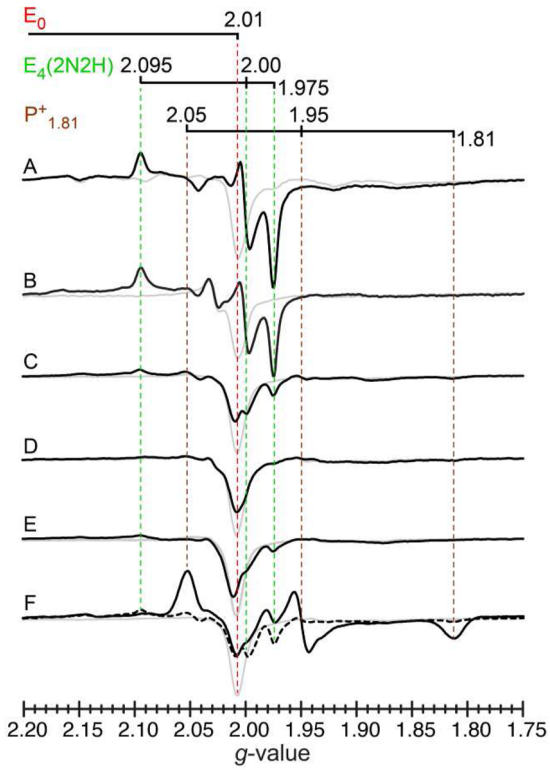

FIG. 2. Effect of CdS preparation, buffer, and illumination temperature and time on photoreduction of QD:MoFe protein complexes. EPR spectra of the S = 1/2, g = 2.0 region are shown identifying signals of the FeMo-co E_0 and E_4(2N2H) states and oxidized P-cluster (P^+) intermediate. Reaction conditions: (a) 50 mM HEPES, pH 7.5, 5 mM NaCl, 5 mM DT, 5 mM MPA, QD1 (sample analyzed in more detail below); 1 atm pN_2; 2 h of illumination at 233 K. (b) 50 mM HEPES, pH 7.5, 5 mM NaCl, 5 mM DT, 5 mM MPA, QD2; 1 atm pN_2; 2 h of illumination at 233 K. (c) 50 mM HEPES, pH 7.5, 200 mM NaCl, 5 mM DT, 5 mM MPA, QD2; 3 atm $p^{15}N_2$; 2 h of illumination at 233 K. (d) 50 mM HEPES, pH 7.5, 200 mM NaCl, 5 mM DT, 5 mM MPA, QD2; 1 atm pN_2; 30 min illumination at 293 K. (e) 50 mM HEPES, pH 7.5, 200 mM NaCl, 5 mM DT, 5 mM MPA, QD2; 1 atm pN_2; 4 W illumination, 1 h at 233 K. (f) 50 mM HEPES, pH 7.5, 200 mM NaCl, 5 mM DT, 5 mM MPA, QD2; 3 atm pN_2; 4 W illumination, at 233 K for 1 h (dotted trace) or 2 h (solid trace). Spectra were collected at P = 1 mW and T = 12 K prior to illumination (gray traces) and post illumination (black traces). All signal intensities were normalized to the E_0 signal intensity at g = 2.01 prior to illumination.

to identify parameters that led to both attenuation of the resting state, E_0, and formation of higher E-states (>E_2) (Fig. 2). Two different concentrations of NaCl were used to create a high (200 mM) or low (5 mM) ionic strength based on binding studies of CdS QDs and the MoFe protein by microscale thermophoresis favoring low salt conditions.[25] Reactions were prepared in an EPR tube under a pN_2 of either 1 or 3 atm to test the pN_2 effect on E-states and equilibrated, in the dark, to a reaction temperature of 233 or 298 K in the integrating sphere (see the supplementary material for details). A comparison of the EPR spectra of the reactions before and after illumination (Fig. 2) showed that the greatest E_0 attenuation and highest level of E_4(2N2H) were observed under

2 W of 405 nm light at 233 K at a NaCl concentration of 5 mM [Figs. 2(a) and 2(b)].

The EPR spectra of samples prepared with either QD1 or QD2 [Figs. 2(a) and 2(b)], were collected after sequential 1 h illumination periods (full spectra, Fig. S3) and simulated using EasySpin[26] to identify and quantify E-state populations (S = 3/2 region, Fig. 3; S = 1/2 region, Fig. 4). At t = 0 in the dark, the QD:MoFe protein spectrum consisted of a nearly uniform E_0 signal at g = 4.33, 3.63, and 2.01,[6,23] with small fractions (2.3% and 6.4%) of signals assigned to the E_2(2H)1c and E_2(2H)1d states, respectively (Table S2). These may have formed from background room light excitation and CdS mediated reduction of the MoFe protein. The result indicates that freezing of the complexes had little to no effect on the integrity of the MoFe protein.

After illumination of the QD1:MoFe protein (and QD2:MoFe protein, Fig. S3) complexes for sequential 1 h periods at 233 K, there was a time-dependent decrease in the intensity of the E_0 signal and appearance of new S = 3/2 and S = 1/2 signals (Figs. 3 and 4, and S3). Simulations of the EPR spectra were used to resolve E-state signals based on comparison to defined Mo-nitrogenase signals (Figs. 3 and 4 and S4 and Tables S2 and S3).[6,8,12,27–29] In addition to E_0, there were signals in the S = 3/2 region (Fig. 3) that match to E_2(2H)1b, E_2(2H)1c, and E_2(2H)1d, which are conformers of the two-electron reduced E_2 state.[12,23] These E_2 states have been proposed to differ in the position of a bridging hydride[12] and vary in population depending on enrichment conditions. E_2(2H)1d has been observed as a major species in CdS:MoFe protein reactions when electron flux was limited by combining low excitation rates in the absence of a hole scavenger.[23] In contrast, the E_2(2H)1b and E_2(2H)1c states are observed in Mo-nitrogenase reactions under high electron flux turnover and have been implicated as intermediates in the N_2 reduction reaction.[8,11]

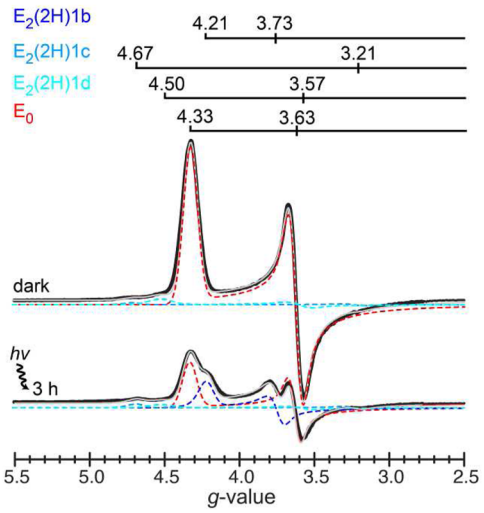

FIG. 3. EPR spectra of the S = 3/2, g = 4.0 region of QD1:MoFe protein complexes before and after 3 h of illumination. EPR spectra (black) and full simulations (gray). The g_x and g_y-values for signal components of the resting state E_0 (red) and conformers of the two-electron reduced E_2 states: E_2(2H)1b (blue), E_2(2H)1c (light blue), and E_2(2H)1d (cyan) (Table S2). EPR spectra collected at P = 1 mW, T = 3.8 K. Reaction conditions, EPR parameters, and spectral simulation details are described in the supplementary material, QD1.

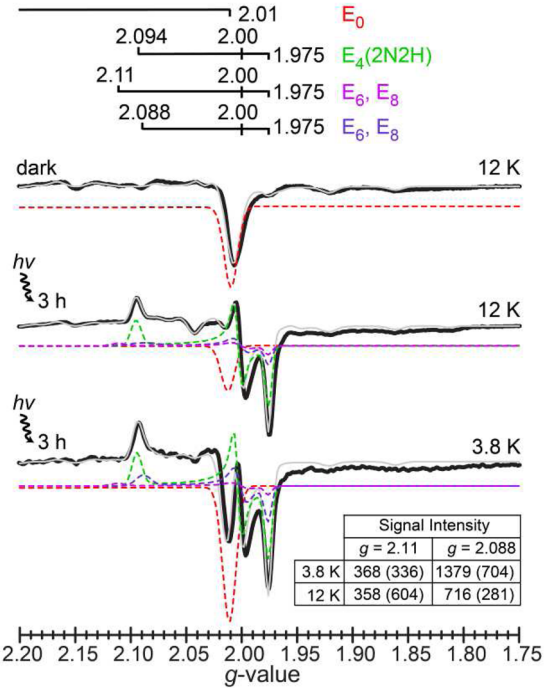

FIG. 4. EPR spectra and simulations of the S = 1/2, g = 2.0 region of QD1:MoFe protein complexes before and after 3 h illumination. EPR spectra (black) and full simulations (gray). Signal components shown for E_0 (red), E_4(2N2H) (green), and signals assigned to E_6 and E_8 conformers[9] (light and dark purple) (Table S3, full simulation Fig. S4). The table intensities of double integrated peak areas for the E_6 and E_8 signals are from simulation of 3.6–3.8 and 12 K spectra of QD1:MoFe protein complexes (numbers in parentheses are from QD2:MoFe protein complexes, Fig. S5). Spectra collected at P = 1 mW and T = 3.8 and 12 K. Reaction conditions, EPR parameters, and spectral simulation are described in the supplementary material, QD1.

The four electron reduced state (E_4) is a key intermediate in the N_2 reduction reaction by nitrogenase. Formation of E_4(4H), which coordinates two bridging hydrides, is required for N_2 binding and activation that results in formation of the E_4(2N2H) state (see Fig. 1). E_4(4H) has been trapped in the MoFe protein under turnover reactions with the Fe protein,[8,28,29] and it has a distinctive S = 1/2 EPR signal at g = 2.15, 2.00, and 1.96 (Table S3).[11,29,30] Weak features identified between g = 2.12 and 2.19 and centered at ~g = 2.15 are consistent with the presence of E_4(4H) for QD1:MoFe protein complexes (Fig. S4, Table S3). These signals showed some variability between samples and were more resolved upon illumination for the sample prepared with QD2 (Fig. S4, Table S3). Reductive elimination of the two hydride ligands from E_4(4H) as a H_2 molecule is a key step for N_2 binding and formation of the E_4(2N2H) intermediate (Fig. 1).[5,8,29] E_4(2N2H) has a distinctive S = 1/2 signal at g = 2.09, 1.99, and 1.97 (Table S3),[29] which was evident following illumination of QD1:MoFe protein (and QD2:MoFe protein) complexes (Fig. 4 and S4). In-line with its formation, spectral simulation after 3 h illumination at 233 K showed an EPR signal

at g = 2.094, 2.00, and 1.975 that matches the g-values and T_{opt} ~12 K of the E_4(2N2H) signal (Fig. 4, Table S3).

In addition to the E_4 state signals in the g = 2.0 region, there were overlapping peaks at g = 2.088–2.11 with distinct temperature dependencies evident from comparing spectra collected at 12 vs 3.6 K (Fig. 4). These spectra were simulated with signals at g = 2.11, 2.00, and 1.975 and g = 2.088, 2.00, and 1.975. For both samples analyzed, the g = 2.088 signal was more clearly dominant at 3.6–3.8 K. For the sample prepared with QD2, the g = 2.11 signal became more intense than the g = 2.088 signal at 12 K (Fig. S5). Slight differences in the behavior of the QD1 spectra relative intensities was observed; however, the g = 2.088 signal was less resolved for this sample compared to that of QD2. Overall, the two signals show similar g-values and similar type temperature-dependencies to a pair of signals at g = 2.11, 2.01, and 1.98 and g = 2.09, 2.01, and 1.98 that were previously observed in the MoFe protein variant H195Q/V70A trapped under turnover with hydrazine (N_2H_4) or diazene (N_2H_2).[9] In that study, the g = 2.09 signal was dominant at lower temperatures (T = 3.8 K), whereas the g = 2.11 signal was dominant at higher temperatures (T = 15 K). Combined ENDOR and HYSCORE studies that used isotopically labeled ^{15}N-substrates assigned the signals to conformers of a E_6 or E_8 state formed after reduction and cleavage of the N–N bond to a –NH_3 ligand (Table S3).[9,31] The similarities between the g = 2.09/2.11 signals in these two systems suggest that illumination of QD:MoFe protein reactions in the frozen state can also trap later E-state intermediates, such as the E_6 and E_8 states observed in the MoFe-protein under reduction by the Fe protein.

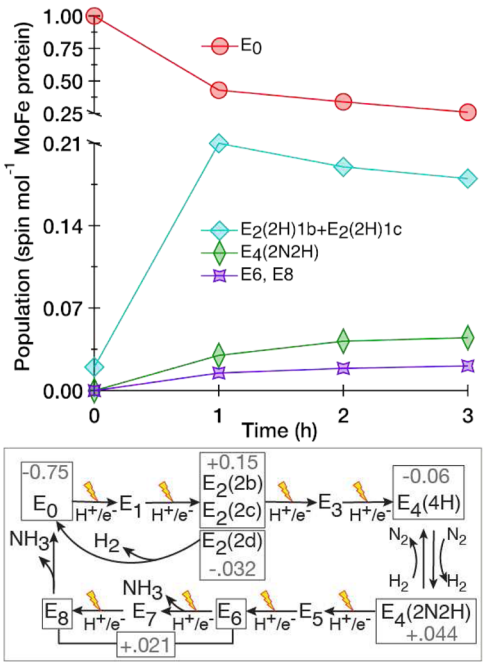

FIG. 5. Top: plots of the changes in the E-state populations in the QD1:MoFe protein complexes following illumination at 233 K. E_0 and E_2 populations are obtained from simulations of 3.8 K spectra (Fig. 3, Table S2). E_4(4H), E_4(2N2H), E_6, and E_8 are derived from simulations of the 12 K spectra (Fig. 4, Table S3). Spin mol^{-1} MoFe protein values are normalized to the initial E_0 spin population at t = 0. Bottom: model of the Lowe–Thorneley E-state intermediates with an increase (+) or decrease (–) in the fractional population of E-states after t = 3 h of illumination at 233 K (gray font).

Using the signal assignments summarized above, the populations of S = 3/2 and S = 1/2 E-states in the reduced MoFe protein were determined by simulation and spin-quantification of the 3.8 and 12 K EPR spectra, respectively (Tables S2 and S3). Figure 5 summarizes the change in populations over the illumination period and maps the final populations onto the Lowe–Thorneley kinetic model. Starting from E_0, 3 h of illumination led to attenuation of ~75% spin mol^{-1} of the resting state, E_0, MoFe protein population. A large fraction of the attenuated E_0 population (31% at t = 1 h; 41% at t = 2 h; 49% at t = 3 h) can be accounted for by reduction to odd-numbered, EPR-silent E-states, i.e., E_1, E_3, E_5, and E_7. The populations of EPR-active E_2, E_4, E_6, and E_8 states varied in proportion according to the reduction level. This is evident by the highest fraction being E_2(2H)1b + E_2(2H)1c that accounted for 21% total spin mol^{-1} MoFe protein at t = 1 h and 18% at t = 3 h. The combined amount of E_2(2H)1c and E_2(2H)1b at all timepoints is similar (18%-21%) but the fractional amounts change over time. This likely reflects differences in the backward relaxation kinetics of H_2 release[12] or kinetics of reduction to higher E-states (Fig. 5, bottom). The trend in the accumulation of E_4(2N2H) was nearly linear and increased from 3% to 4.4% of the total spin population. The formation of E_2, E_4(4H), and E_4(2N2H) signifies that performing photochemical reactions at 233 K supports proton and electron transfer, as well as N_2 binding and reduction, by the MoFe protein. A low population of E_6 and E_8 state signals was detected in the 12 K spectrum, increasing from 1.5% to 2.1% spin mol^{-1} MoFe protein over the 1–3 h period of illumination.

CONCLUSIONS

Overall, this work demonstrates that nanocrystal-MoFe protein complexes can be used in combination with illumination in the frozen state to populate higher E-states of the FeMo-cofactor catalytic cycle in a single sample. Combining the approach developed here with inhibitory studies and MoFe protein mutagenesis can enable future studies directed at understanding specific determinants of E-state equilibrium in mechanism. These approaches may help to support greater enrichment of higher E-states (i.e., E6 and E8) that have been challenging to isolate in nitrogenase under N_2 reduction conditions and determination of E-state kinetics of nitrogenase, which have proved challenging to address with the natural biochemical system.

SUPPLEMENTARY MATERIAL

The supplementary material section includes materials and methods with descriptions of CdS Quantum Dot (QD) synthesis, MoFe protein preparation, photochemical $^{15}NH_3$ production assays, nuclear magnetic resonance spectroscopy, nuclear magnetic resonance spectroscopy analysis, electron paramagnetic resonance spectroscopy, and EPR simulations and E-state population analysis. It also contains Fig. S1—UV–Vis absorption spectrum normalized at the first exciton peak of QDs, Fig. S2—^{1}H-NMR spectra of QD2:MoFe protein reactions, Fig. S3—EPR spectra of QD:MoFe

protein complexes, Fig. S4—EPR spectra of the S = 1/2, g = 2.0 region of QD:MoFe protein complexes, Fig. S5—EPR spectra collected at 3.6 and 12 K and simulations of the S = 1/2, g = 2.0 region of QD2:MoFe protein complexes, Table S1—fluorometric and ^{1}H-NMR measurements of NH_3 production by QD:MoFe protein reactions, Table S2—EPR signals and spin concentrations for S = 3/2 region for Fe protein:MoFe protein and QD:MoFe protein reactions, and Table S3—EPR signals of S = 1/2 region for Fe protein:MoFe protein and QD:MoFe protein reactions.

ACKNOWLEDGMENTS

Funding was provided by the U.S. Department of Energy (DOE), Office of Science, Basic Energy Sciences, Chemical Sciences, Geosciences, and Biosciences Division. This work was authored, in part, by the Alliance for Sustainable Energy, LLC, the manager and operator of the National Renewable Energy Laboratory for the U.S. Department of Energy (DOE) under Contract No. DEAC36-08GO28308. The U.S. Government and the publisher, by accepting the article for publication, acknowledge that the U.S. Government retains a nonexclusive, paid-up, irrevocable, worldwide license to publish or reproduce the published form of this work, or allow others to do so, for U.S. Government purposes. The authors gratefully acknowledge the NREL NMR facility and Dr. Renee Happs for assistance with NMR spectroscopy measurements of $^{15}NH_3$ in photochemical reactions.

AUTHOR DECLARATIONS

Conflict of Interest

The authors have no conflicts to disclose.

Author Contributions

The manuscript was written through contributions of all authors. All authors have given approval to the final version of the manuscript.

L.M.P., G.E.V., B.C., Z.-Y.Y., and D.W.M contributed equally to the work.

Lauren M. Pellows: Data curation (equal); Formal analysis (supporting); Methodology (supporting); Resources (equal); Writing – review & editing (supporting). **Gregory E. Vansuch**: Conceptualization (equal); Data curation (equal); Formal analysis (equal); Funding acquisition (lead); Investigation (equal); Methodology (equal); Project administration (equal); Supervision (lead); Writing – original draft (lead); Writing – review & editing (equal). **Bryant Chica**: Conceptualization (equal); Formal analysis (supporting); Investigation (supporting); Methodology (supporting); Writing – review & editing (supporting). **Zhi-Yong Yang**: Formal analysis (supporting); Methodology (supporting); Resources (equal); Writing – review & editing (supporting). **Jesse L. Ruzicka**: Data curation (equal); Formal analysis (equal); Methodology (equal); Project administration (supporting); Resources (equal); Supervision (supporting); Writing – original draft (equal); Writing – review & editing (equal). **Mark A. Willis**: Data curation (equal); Formal analysis (supporting); Investigation (supporting); Methodology (supporting); Resources (equal); Writing – review & editing (supporting). **Andrew Clinger**: Data curation (supporting). **Katherine A. Brown**: Conceptualization (equal); Investigation (supporting); Methodology (supporting); Writing – review & editing (supporting). **Lance C. Seefeldt**: Conceptualization (equal); Funding acquisition (equal); Investigation (supporting); Project administration (equal); Resources (equal); Writing – review & editing (supporting). **John W. Peters**: Conceptualization (equal); Funding acquisition (equal); Methodology (supporting); Project administration (equal); Resources (supporting); Supervision (equal); Writing – review & editing (equal). **Gordana Dukovic**: Conceptualization (equal); Formal analysis (equal); Funding acquisition (equal); Methodology (equal); Project administration (equal); Resources (equal); Supervision (equal); Writing – review & editing (supporting). **David W. Mulder**: Data curation (equal); Formal analysis (lead); Investigation (equal); Methodology (equal); Project administration (supporting); Supervision (supporting); Writing – original draft (equal); Writing – review & editing (equal). **Paul W. King**: Conceptualization (equal); Formal analysis (supporting); Funding acquisition (lead); Investigation (equal); Methodology (equal); Project administration (equal); Resources (equal); Supervision (lead); Writing – original draft (lead); Writing – review & editing (equal).

DATA AVAILABILITY

The data that support the findings of this study are available from the corresponding authors upon reasonable request.

NOMENCLATURE

^{1}H-NMR	proton nuclear magnetic resonance
atm	atmosphere
ATP	adenosine triphosphate
CdS	cadmium sulfide
e^-	electron
EPR	electron paramagnetic resonance
E_0, E_2, E_4, E_6, E_8	catalytic intermediates of the MoFe protein
FeMo-co	MoFe protein iron molybdenum cofactor
Fe protein	nitrogenase iron protein
h	hour
h^+	hole
H	proton
H_2	hydrogen gas
k_{EA}	rate constant of electron accumulation
K	kelvin
MoFe protein	nitrogenase iron molybdenum protein
mW	milliwatt
N_2	nitrogen gas
NH_3	ammonia
P	power
P-cluster	MoFe protein [8Fe–7S] cluster
QEET	quantum efficiency of electron transfer
QD	quantum dot
t	time
T	temperature
W	watt

REFERENCES

[1]F. B. Simpson and R. H. Burris, "A nitrogen pressure of 50 atmospheres does not prevent evolution of hydrogen by nitrogenase," Science **224**(4653), 1095–1097 (1984).

[2]L. C. Seefeldt, J. W. Peters, D. N. Beratan, B. Bothner, S. D. Minteer, S. Raugei, and B. M. Hoffman, "Control of electron transfer in nitrogenase," Curr. Opin. Chem. Biol. **47**, 54–59 (2018).

[3]Z.-Y. Yang, A. Badalyan, B. M. Hoffman, D. R. Dean, and L. C. Seefeldt, "The Fe protein cycle associated with nitrogenase catalysis requires the hydrolysis of two ATP for each single electron transfer event," J. Am. Chem. Soc. **145**(10), 5637–5644 (2023).

[4]D. J. Lowe, R. R. Eady, and R. N. F. Thorneley, "Electron-paramagnetic-resonance studies on nitrogenase of *Klebsiella pneumoniae*. Evidence for acetylene- and ethylene-nitrogenase transient complexes," Biochem. J. **173**(1), 277–290 (1978).

[5]L. C. Seefeldt, Z.-Y. Yang, D. A. Lukoyanov, D. F. Harris, D. R. Dean, S. Raugei, and B. M. Hoffman, "Reduction of substrates by nitrogenases," Chem. Rev. **120**(12), 5082–5106 (2020).

[6]B. M. Barney, D. Lukoyanov, R. Y. Igarashi, M. Laryukhin, T.-C. Yang, D. R. Dean, B. M. Hoffman, and L. C. Seefeldt, "Trapping an intermediate of dinitrogen (N_2) reduction on nitrogenase," Biochemistry **48**(38), 9094–9102 (2009).

[7]J. Christiansen, P. J. Goodwin, W. N. Lanzilotta, L. C. Seefeldt, and D. R. Dean, "Catalytic and biophysical properties of a nitrogenase apo-MoFe protein produced by a *nifB*-deletion mutant of *Azotobacter vinelandii*," Biochemistry **37**(36), 12611–12623 (1998).

[8]D. Lukoyanov, B. M. Barney, D. R. Dean, L. C. Seefeldt, and B. M. Hoffman, "Connecting nitrogenase intermediates with the kinetic scheme for N_2 reduction by a relaxation protocol and identification of the N_2 binding state," Proc. Natl. Acad. Sci. U. S. A. **104**(5), 1451–1455 (2007).

[9]D. Lukoyanov, S. A. Dikanov, Z.-Y. Yang, B. M. Barney, R. I. Samoilova, K. V. Narasimhulu, D. R. Dean, L. C. Seefeldt, and B. M. Hoffman, "ENDOR/HYSCORE studies of the common intermediate trapped during nitrogenase reduction of N_2H_2, CH_3N_2H, and N_2H_4 support an alternating reaction pathway for N_2 reduction," J. Am. Chem. Soc. **133**(30), 11655–11664 (2011).

[10]D. Lukoyanov, Z.-Y. Yang, S. Duval, K. Danyal, D. R. Dean, L. C. Seefeldt, and B. M. Hoffman, "A confirmation of the quench-cryoannealing relaxation protocol for identifying reduction states of freeze-trapped nitrogenase intermediates," Inorg. Chem. **53**(7), 3688–3693 (2014).

[11]D. Lukoyanov, Z.-Y. Yang, N. Khadka, D. R. Dean, L. C. Seefeldt, and B. M. Hoffman, "Identification of a key catalytic intermediate demonstrates that nitrogenase is activated by the reversible exchange of N_2 for H_2," J. Am. Chem. Soc. **137**(10), 3610–3615 (2015).

[12]D. A. Lukoyanov, N. Khadka, Z.-Y. Yang, D. R. Dean, L. C. Seefeldt, and B. M. Hoffman, "Hydride conformers of the nitrogenase FeMo-cofactor two-electron reduced state E_2(2H), assigned using cryogenic intra electron paramagnetic resonance cavity photolysis," Inorg. Chem. **57**(12), 6847–6852 (2018).

[13]S. Maritano, S. A. Fairhurst, and R. R. Eady, "Novel EPR signals associated with FeMoco centres of MoFe protein in MgADP-inhibited turnover of nitrogenase," FEBS Lett. **505**(1), 125–128 (2001).

[14]S. Shaw, D. Lukoyanov, K. Danyal, D. R. Dean, B. M. Hoffman, and L. C. Seefeldt, "Nitrite and hydroxylamine as nitrogenase substrates: Mechanistic implications for the pathway of N_2 reduction," J. Am. Chem. Soc. **136**(36), 12776–12783 (2014).

[15]S. Raugei, L. C. Seefeldt, and B. M. Hoffman, "Critical computational analysis illuminates the reductive-elimination mechanism that activates nitrogenase for N_2 reduction," Proc. Natl. Acad. Sci. U. S. A. **115**(45), E10521–E10530 (2018).

[16]R. N. Thorneley and D. J. Lowe, "Kinetics and mechanism of the nitrogenase enzyme system," in *Molybdenum Enzymes*, Metal Ions in Biology Series, edited by T. G. Spiro (Wiley-Interscience Publications, New York, 1985), Vol. 7, pp. 221–284.

[17]K. A. Brown, D. F. Harris, M. B. Wilker, A. Rasmussen, N. Khadka, H. Hamby, S. Keable, G. Dukovic, J. W. Peters, L. C. Seefeldt, and P. W. King, "Light-driven dinitrogen reduction catalyzed by a CdS:nitrogenase MoFe protein biohybrid," Science **352**(6284), 448–450 (2016).

[18]K. A. Brown, J. Ruzicka, H. Kallas, B. Chica, D. W. Mulder, J. W. Peters, L. C. Seefeldt, G. Dukovic, and P. W. King, "Excitation-rate determines product stoichiometry in photochemical ammonia production by CdS quantum dot-nitrogenase MoFe protein complexes," ACS Catal. **10**(19), 11147–11152 (2020).

[19]B. Chica, J. Ruzicka, L. M. Pellows, H. Kallas, E. Kisgeropoulos, G. E. Vansuch, D. W. Mulder, K. A. Brown, D. Svedruzic, J. W. Peters, G. Dukovic, L. C. Seefeldt, and P. W. King, "Dissecting electronic-structural transitions in the nitrogenase MoFe protein P-cluster during reduction," J. Am. Chem. Soc. **144**(13), 5708–5712 (2022).

[20]J. L. Ruzicka, L. M. Pellows, H. Kallas, K. E. Shulenberger, O. A. Zadvornyy, B. Chica, K. A. Brown, J. W. Peters, P. W. King, L. C. Seefeldt, and G. Dukovic, "The kinetics of electron transfer from CdS nanorods to the MoFe protein of nitrogenase," J. Phys. Chem. C **126**(19), 8425–8435 (2022).

[21]J. K. Utterback, M. B. Wilker, D. W. Mulder, P. W. King, J. D. Eaves, and G. Dukovic, "Quantum efficiency of charge transfer competing against non-exponential processes: The case of electron transfer from CdS nanorods to hydrogenase," J. Phys. Chem. C **123**(1), 886–896 (2019).

[22]M. B. Wilker, K. E. Shinopoulos, K. A. Brown, D. W. Mulder, P. W. King, and G. Dukovic, "Electron transfer kinetics in CdS nanorod–[FeFe]-Hydrogenase complexes and implications for photochemical H_2 generation," J. Am. Chem. Soc. **136**(11), 4316–4324 (2014).

[23]B. Chica, J. Ruzicka, H. Kallas, D. W. Mulder, K. A. Brown, J. W. Peters, L. C. Seefeldt, G. Dukovic, and P. W. King, "Defining intermediates of nitrogenase MoFe protein during N_2 reduction under photochemical electron delivery from CdS quantum dots," J. Am. Chem. Soc. **142**(33), 14324–14330 (2020).

[24]G. E. Vansuch, D. W. Mulder, B. Chica, J. L. Ruzicka, Z.-Y. Yang, L. M. Pellows, M. A. Willis, K. A. Brown, L. C. Seefeldt, J. W. Peters, G. Dukovic, and P. W. King, "Cryo-annealing of photoreduced CdS quantum dot–nitrogenase MoFe protein complexes reveals the kinetic stability of the E_4(2N_2H) intermediate," J. Am. Chem. Soc. **145**(39), 21165–21169 (2023).

[25]L. M. Pellows, M. A. Willis, J. L. Ruzicka, B. P. Jagilinki, D. W. Mulder, Z. Y. Yang, L. C. Seefeldt, P. W. King, G. Dukovic, and J. W. Peters, "High affinity electrostatic interactions support the formation of CdS quantum dot:nitrogenase MoFe protein complexes," Nano Lett. **23**, 10466–10472 (2023).

[26]S. Stoll and A. Schweiger, "EasySpin, a comprehensive software package for spectral simulation and analysis in EPR," J. Magn. Reson. **178**(1), 42–55 (2006).

[27]R. Y. Igarashi, M. Laryukhin, P. C. Dos Santos, H.-I. Lee, D. R. Dean, L. C. Seefeldt, and B. M. Hoffman, "Trapping H-bound to the nitrogenase FeMo-cofactor active site during H_2 evolution: Characterization by ENDOR spectroscopy," J. Am. Chem. Soc. **127**(17), 6231–6241 (2005).

[28]D. Lukoyanov, N. Khadka, Z.-Y. Yang, D. R. Dean, L. C. Seefeldt, and B. M. Hoffman, "Reversible photoinduced reductive elimination of H_2 from the nitrogenase dihydride state, the E_4(4H) Janus intermediate," J. Am. Chem. Soc. **138**(4), 1320–1327 (2016).

[29]D. Lukoyanov, N. Khadka, Z.-Y. Yang, D. R. Dean, L. C. Seefeldt, and B. M. Hoffman, "Reductive elimination of H_2 activates nitrogenase to reduce the N≡N triple bond: Characterization of the E_4(4H) Janus intermediate in wild-type enzyme," J. Am. Chem. Soc. **138**(33), 10674–10683 (2016).

[30]Z.-Y. Yang, N. Khadka, D. Lukoyanov, B. M. Hoffman, D. R. Dean, and L. C. Seefeldt, "On reversible H_2 loss upon N_2 binding to FeMo-cofactor of nitrogenase," Proc. Natl. Acad. Sci. U. S. A. **110**(41), 16327–16332 (2013).

[31]D. Lukoyanov, Z.-Y. Yang, B. M. Barney, D. R. Dean, L. C. Seefeldt, and B. M. Hoffman, "Unification of reaction pathway and kinetic scheme for N_2 reduction catalyzed by nitrogenase," Proc. Natl. Acad. Sci. U. S. A. **109**(15), 5583–5587 (2012).